Journal of Modern Optics
Vol. 00, No. 00, DD Month 200x, 1–8

Remotely prepared single-photon time-encoded ebits: homodyne tomography characterization

MILENA D'ANGELO*,† , ALESSANDRO ZAVATTA‡, VALENTINA PARIGI†, MARCO BELLINI†,‡
† European Laboratory for Non-Linear Spectroscopy, Via N. Carrara 1, 50019 Sesto Fiorentino, Florence, Italy
‡ Istituto Nazionale di Ottica Applicata-CNR, L.go E. Fermi, 6, I-50125, Florence, Italy
(Received 00 Month 200x; In final form 00 Month 200x)

We propose and experimentally verify a novel method for the remote preparation of entangled bits (ebits) made of a single photon coherently delocalized between two well-separated temporal modes. The proposed scheme represents a remotely tunable source for tailoring arbitrary ebits, whether maximally or non-maximally entangled, which is highly desirable for applications in quantum information technology. The remotely prepared ebit is studied by performing two-mode homodyne tomography with an ultra-fast time-domain balanced homodyne detection scheme recently developed in our laboratory.

Keywords: Single-photon entanglement; Quantum tomography

1 Introduction

Entanglement, nonlocal correlations, indistinguishable alternatives are, historically, among the most intriguing and appealing topics of quantum mechanics. Besides their relevance in fundamental physics (EPR paradox [1], Bell's inequality tests [2]), these phenomena have attracted much attention due to their usefulness in quantum information technology. Extravagant but promising protocols such as quantum teleportation, quantum cryptography, and quantum computation have been proposed and experimentally verified (see e.g. [3] and references therein). Both quantum information protocols and Bell's inequality tests were originally based on two-photon entangled states.

Increasing attention has recently been given to a new quantum information perspective: the carriers of quantum information are no longer the photons, but rather the spatiotemporal field modes "carrying" them. The first steps in this direction were taken by Tan, Walls, and Collet (TWC) [4]: when a single photon impinges on a beam-splitter whose outputs are described by the spatial modes A and B, the emerging single photon is described by the state $|\psi\rangle = \alpha|1\rangle_A|0\rangle_B + \beta|0\rangle_A|1\rangle_B$, where $|0\rangle$ is the vacuum, $|1\rangle$ is a single-photon Fock state, and α and β are complex amplitudes such that $|\alpha|^2 + |\beta|^2 = 1$. Based on this perspective, the concept of entanglement can be extended to any system containing a fixed number $(n = 1, 2, ..)$ of photons, provided at least one pair of spatiotemporal modes is involved. For $n = 1$, for instance, one may have a "single-photon N-mode entangled" system, with $N \geq 2$.

The formal analogy between TWC single-photon state and Bohm-like two-photon polarization entangled state has inspired several practical applications [5–7]. However, intensive debates are still dedicated to the possibility of extending both the concepts of entanglement and nonlocality to TWC-type single-photon systems (see e.g. [8–12]). On the one hand, the main criticisms against such extension are the following: 1) by writing the TWC single-photon state as $|\psi\rangle = (\alpha a_A^\dagger + \beta a_B^\dagger)|0\rangle$, the entanglement disappears; 2) the TWC single-photon state is nothing else but the state characterizing a single photon in the first half of an interferometer, and since the interference at the single-photon level is already understood in terms of wave-particle duality, the introduction of the concept of single-photon two-mode entanglement is unnecessary. On the other hand, the correlations between two (or more) well separated field modes

*dangelo@lens.unifi.it

carrying a single photon have been shown to be nonclassical [4,9,10]. This has naturally lead to talk about single-photon N-mode entanglement and to start proposing Bell-type nonlocality tests; such single-photon nonlocality tests would consist in performing simultaneous measurements (at separate locations) on the pair of entangled spatiotemporal modes carrying the delocalized single photon and then check wether the correlations between them violate a Bell-type locality condition. This line of thought could explain single-photon interference effects without requiring the counterintuitive wave-particle duality.

In this paper, we propose a remotely tunable source of TWC-like single-photon states, namely [13]:

$$|\Psi\rangle = \alpha|1^{(n)}\rangle|0^{(n+1)}\rangle + \beta|0^{(n)}\rangle|1^{(n+1)}\rangle, \tag{1}$$

where n and $n+1$ denote two co-propagating but non-overlapping temporal modes or time-bins. After clarifying the working principle of our source, we describe its experimental implementation and show its two-mode quantum homodyne tomography characterization: by performing two-mode time-domain balanced homodyne detection on the pair of well separated time-bins, we reconstruct both density matrix and Wigner function of the system emitted by our source. The experimentally reconstructed density matrix is in very good agreement with the expected state of Eq.(1). Furthermore, the reconstructed two-mode Wigner function explicitly shows some peculiar characteristics of the remotely generated system: the existence of both a fixed *relative* phase and strong correlations between the two separate time bins carrying the delocalized single photon. We thus refer to the time-domain single-photon two-mode states of Eq.(1) as time-encoded entangled bits (ebits). It is certainly a very delicate matter to make a clear distinction between the concept of entanglement at the single-photon (corpuscular) level and the classical concept of (wave) interference. We plan to treat this topic more extensively elsewhere; at the moment, we have limited our studies to the implementation and characterization of the proposed source.

From the applicative viewpoint, our scheme may find immediate application in quantum information technology. In fact, single-photon ebits have been proven to enable linear optics quantum teleportation [5] and play a central role in linear optics quantum computation [6,7]. In addition, the time-bin encoding of quantum information, recently developed by Gisin's group on the line of Franson's approach [14], has proved its superior robustness against decoherence when long-distance applications are involved [15], which is, when the insensitivity to both depolarization and polarization fluctuations becomes a strong requirement. Furthermore, since the carriers of entanglement are naturally separated (i.e. no further optical element is required) and undergo the same losses, entanglement in time is less sensitive to losses and easier to purify [16]. Thus, although the delocalization of a single photon between two separate spatial modes is the most intuitive and conceptually simple experiment to realize, its time-domain dual is probably even more appealing, both from the fundamental and the applicative viewpoints.

2 Working principle

Our idea is to exploit the spontaneous parametric down conversion (SPDC) signal-idler pairs [17] generated by a train of phase-locked pump pulses [15,18] and an unbalanced Michelson interferometer inserted in the idler channel, to generate indistinguishability between two signal single-photon two-mode states, namely $|1^{(n)}\rangle|0^{(n+1)}\rangle$ and $|0^{(n)}\rangle|1^{(n+1)}\rangle$.

To this end, we set the interferometer delay T equal to the fixed inter-pulse separation T_p characterizing the train of pump pulses; in this configuration, a click in the idler (trigger) channel may be caused by either one of the following indistinguishable events: i) the idler belonging to the biphoton generated by the n^{th} pump pulse reached the trigger detector after propagating through the long arm of the interferometer; ii) the idler belonging to the biphoton generated by the $(n+1)^{th}$ pump pulse reached the trigger detector after propagating through the short arm of the interferometer. For an infinite train of phase-locked pump pulses, a click in the trigger detector should remotely delocalize the corresponding signal photon between two co-propagating but well-separated time-bins.

Based on a standard quantum mechanical calculation, we find that the combination of indistinguishability and tight filtering in the idler channel guarantees the conditional remote preparation, in the signal

channel, of the temporally delocalized single-photon ebit:

$$|\Psi^{\phi_i}\rangle_s = \frac{1}{\sqrt{2}}(|1^{(n)}\rangle_s|0^{(n+1)}\rangle_s + e^{-i\phi_i}|0^{(n)}\rangle_s|1^{(n+1)}\rangle_s), \tag{2}$$

with $\phi_i = \Omega_p T_p - \Omega_i T$, with Ω_p and Ω_i the central frequencies of pump and idler beams, respectively. Interestingly, the relative phase ϕ_i characterizing the remotely prepared ebit is defined not only by the phase difference introduced by the Michelson interferometer ($\varphi_{int} = \Omega_i T$), but also by the relative phase between consecutive pump pulses ($\varphi_{pump} = \Omega_p T_p$). Similar to many SPDC experiments, this effect can be intuitively understood in terms of Klyshko's advanced-wave model [17, 19].

The result of Eq. (2) represents the temporal counterpart of the spatially delocalized single photon produced at the output ports of a beam splitter, which has been experimentally studied by Babichev, *et al.* [9]. However, the effect behind these two sources of delocalized single-photon two-mode states is quite different; this is emphasized by the fact that, different from Ref. [9], the entangled state of Eq. (2) is prepared remotely, without performing any manipulation on the signal photons.

In particular, our scheme exploits the coherence of the SPDC process: the SPDC bi-photon, considered as a whole, retains the coherence of the pump beam and, in particular, the phase-locking characterizing the train of pump pulses [14, 15]. If no conditioning measurements are performed in the idler arm, the signal beam alone is chaotic, namely, it is made up of an incoherent superposition of pulses, all independent of each other. To rebuild coherence between consecutive non-overlapping signal temporal modes (as described by Eq. (2)), our scheme exploits, first, the phase-locking characterizing both the train of pump pulses and the produced train of SPDC biphoton, and, second, the indistinguishability (generated by the remote interferometer) between the events leading to a click in the idler channel.

An important advantage of our remote state preparation scheme is the possibility of generating both maximally and non-maximally single-photon entangled states, with any relative phase ϕ_i, by performing simple and reversible operations in the idler arm (or on the train of pump pulses). For instance, two of the four Bell states, namely $|\Psi^{\pm}\rangle_s = \frac{1}{\sqrt{2}}(|1^{(n)}\rangle_s|0^{(n+1)}\rangle_s \pm |0^{(n)}\rangle_s|1^{(n+1)}\rangle_s)$, can be easily generated by manipulating the interferometer. Furthermore, the probability amplitudes characterizing the delocalized single photon may be continuously varied by simply introducing controllable losses in one arm of the interferometer; this has the only effect of lowering the production rate but does not introduce any impurity in the state generated in the signal channel.

3 Experimental implementation

The experimental setup is pictured in Fig. 1. The 1.5 ps pulses at 786 nm from a mode-locked Ti:Sapphire laser at a repetition rate of 82 MHz are frequency doubled in a LBO crystal. The resulting pulse train impinges on a non-linear BBO crystal cut for degenerate ($\Omega_s = \Omega_i = \Omega_p/2$) non-collinear type-I SPDC; signal-idler photon pairs centered around 786 nm are thus generated in two distinct spatial modes. A single-mode fiber and a pair of etalon interference filters (F) are employed for spatial and spectral filtering of the idler beam before its entrance in a fiber-coupled piezo-controlled (PZT) Michelson interferometer; a single-photon detector (D_1) is inserted at the exit port of the interferometer. The signal beam propagates in free space before being mixed at a 50-50 beam-splitter (BS) with a local oscillator (LO) for high-frequency time-domain balanced homodyne detection (HD) [20, 21].

Spatial and spectral filtering of the idler mode guarantees the conditional projection of the signal photons into a single-photon pure state [22–24]. On the other hand, the Michelson interferometer generates indistinguishability between two consecutive temporal modes propagating in the idler channel: an idler photon detected by D_1 may have been generated by either the n^{th} or the $(n+1)^{th}$ pump pulse, provided that the time delay (T) between the short and long arms of the interferometer is chosen to be approximately equal to the time separation between two consecutive pump pulses ($T_p = 12.3$ ns). Notice that the bandpass of the spectral filter in the idler arm ($\sigma_i = 50$ GHz) is wide enough so that no first order interference occurs ($\sigma_i \gg \pi/T_p$). The existence of first order interference at the exit of the interferometer, in the idler arm, would not allow generating the desired state of Eq.(2) in the signal channel.

4 Tomographic characterization

In order to characterize our source, we perform quantum homodyne tomography: both the density matrix and the Wigner function of the prepared system can be reconstructed from the two-mode homodyne data, namely, from the joint distribution of the field quadratures X_1 and X_2 associated with each one of the two time bins carrying the delocalized single photon [9]. In fact, quantum homodyne tomography allows gaining complete information about the system under investigation; different from photon counting experiments, homodyne detection is sensitive to phase information and allows monitoring both experimental losses (i.e., the vacuum contribution) and multi-photon contributions. The direct measurement of such joint distribution ($p(X_1(\theta_1), X_2(\theta_2))$, where θ_i is the phase of the local oscillator spatially and temporally matched with the $i = 1, 2$ mode) is made possible by the ultrafast time-domain homodyne detection scheme recently developed in our laboratory [21, 25].

4.1 *Theoretical predictions*

The Wigner function for a two-mode state is given by [26]:

$$W(x_1, y_1; x_2, y_2) = \frac{4}{\pi^2} \int d\chi_1 d\chi_2 e^{-4iy_1\chi_1} e^{-4iy_2\chi_2} \langle x_1 + \chi_1, x_2 + \chi_2 | \hat{\rho} | x_1 - \chi_1, x_2 - \chi_2 \rangle, \tag{3}$$

where x_i and y_i are the field quadratures associated with the i mode ($i = 1, 2$), and correspond to the quadrature operators $\hat{x}_i = (\hat{a}_i + \hat{a}_i^\dagger)/2$ and $\hat{y}_i = i(\hat{a}_i^\dagger - \hat{a}_i)/2$; $\hat{\rho}$ is the density matrix of the system to be measured.

The Wigner function associated with the delocalized single photon of Eq. (2) is given by:

$$W(x_1, y_1; x_2, y_2) = \frac{1}{2}[W_1(x_1, y_1)W_0(x_2, y_2) \; + \; W_0(x_1, y_1)W_1(x_2, y_2) + 8W_{10}(x_1, y_1; x_2, y_2)], \tag{4}$$

where $W_1(x, y) = \frac{2}{\pi} e^{-2x^2} e^{-2y^2} (4x^2 + 4y^2 - 1)$ and $W_0(x, y) = \frac{2}{\pi} e^{-2x^2} e^{-2y^2}$ are the single-mode Wigner functions associated with a single-photon Fock state and with the vacuum, respectively; on the other hand, $W_{10}(x_1, y_1; x_2, y_2)$ is a non-factorable 4-D function which couples the quadratures of the two consecutive temporal modes carrying the delocalized single photon:

$$W_{10}(x_1, y_1; x_2, y_2) = W_0(x_1, y_1)W_0(x_2, y_2) \; [cos\phi_i(x_1x_2 + y_1y_2) + sin\phi_i(y_1x_2 - y_2x_1)]. \tag{5}$$

Equations (4) and (5) indicate that the Wigner function associated with the delocalized signal photon contains information about its characteristic relative phase ϕ_i. In particular, based on the phase delay

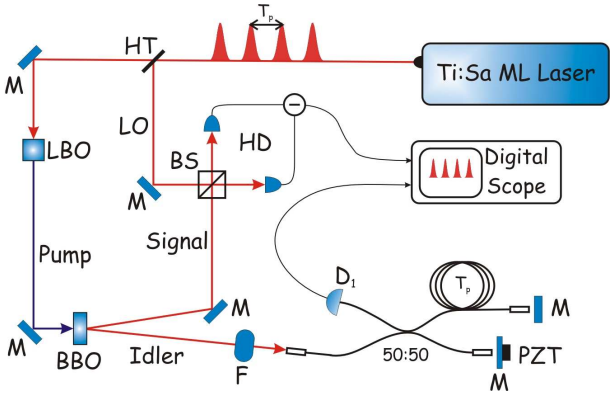

Figure 1. Schematic representation of the experimental setup. 50:50 is a 3 dB fiber coupler, HT a high-transmission beam splitter, and M are mirrors.

introduced by the interferometer in the idler arm, either correlation or anti-correlation arises between the quadratures of two otherwise independent signal temporal modes.

Interestingly, the 4-D Wigner function of Eq. (4) factors when written in terms of the phase-dependent coupled quadratures [26]: $x_A^{\phi_i} = (x_1 + x_2^{\phi_i})/\sqrt{2}$, $x_B^{\phi_i} = (x_1 - x_2^{\phi_i})/\sqrt{2}$, $y_A^{\phi_i} = (y_1 + y_2^{\phi_i})/\sqrt{2}$, $y_B^{\phi_i} = (y_1 - y_2^{\phi_i})/\sqrt{2}$, where we have defined $x_2^{\phi_i} = x_2 cos\phi_i - y_2 sin\phi_i$ and $y_2^{\phi_i} = x_2 sin\phi_i + y_2 cos\phi_i$, reducing to $W(x_A^{\phi_i}, y_A^{\phi_i}; x_B^{\phi_i}, y_B^{\phi_i}) = W_1(x_A^{\phi_i}, y_A^{\phi_i}) W_0(x_B^{\phi_i}, y_B^{\phi_i})$. Of course, the specific linear combinations of the quadratures (x_1, y_1, x_2, y_2), which allows factorizing the two-mode Wigner function depends on the relative phase ϕ_i characterizing the delocalized single photon of Eq. (2). For instance, for $\phi_i = 0$, we have:

$$W^{\phi_i=0}(x_1, y_1; x_2, y_2) = W_1(\frac{x_1 + x_2}{\sqrt{2}}, \frac{y_1 + y_2}{\sqrt{2}}) W_0(\frac{x_1 - x_2}{\sqrt{2}}, \frac{y_1 - y_2}{\sqrt{2}}). \quad (6)$$

This result explicitly indicates that the delocalized single photon cannot be described in terms of the quadratures associated with neither one of the two distant temporal modes (1 and 2), separately; however, the single photon is well defined in the phase space of the center of mass $((x_1 + x_2)/\sqrt{2}, (y_1 + y_2)/\sqrt{2})$, while in the phase space $((x_1 - x_2)/\sqrt{2}, (y_1 - y_2)/\sqrt{2})$ only the vacuum is defined. Thus, the 4-D Wigner function is expected to reproduce the correlations remotely generated between pairs of well-separated signal temporal modes carrying a delocalized single photon.

4.2 *Experimental measurements and results*

In order to characterize the remotely prepared system, we perform two-mode quantum homodyne detection and employ quantum tomography to reconstruct both its two-mode density matrix and its two-mode Wigner function. In particular, the density matrix elements are reconstructed by averaging the corresponding pattern functions over all the homodyne data [26, 27]; the reconstructed density matrix, without any vacuum removal, is then used to reconstruct the two-mode Wigner function (for more details see [21, 25]).

The reconstruction of the two-mode Wigner function of Eq. (4) would normally require the measurement of the joint marginal distribution of the quadratures $X_1(\theta_1) = x_1 \cos\theta_1 - y_1 \sin\theta_1$ and $X_2(\theta_2) = x_2 \cos\theta_2 - y_2 \sin\theta_2$, for different values of the phases θ_1 and θ_2 of two LO pulses spatially and temporally matched (i.e. synchronized) to the signal temporal modes 1 and 2, respectively. In our case, the measurement process is simplified by the fact that the two-mode delocalized single photon has a completely undefined total phase $\theta_1 + \theta_2$; hence, only the relative phase $\Delta\theta = \theta_1 - \theta_2$ needs to be controlled in the experiment [9, 26]. In other words, we expect the joint marginal distribution $p(X_1, X_2, \theta_1, \theta_2)$ to be $p(X_1, X_2, \Delta\theta)$.

Moreover, the joint marginal distribution associated with the single-photon time-encoded ebit of Eq. (4) ($p(X_1, X_2, \Delta\theta, \phi_i)$), is invariant under interchange of ϕ_i and $\Delta\theta$. We exploit this property for overcoming the difficulty connected to the generation of a pair of phase-controllable LO pulses out of the train coming from the laser. Rather than varying the relative LO phase, one may keep $\Delta\theta$ fixed (by just using any two consecutive pulses directly from the mode-locked laser) and vary the relative phase ϕ_i by means of the interferometer. Although what we actually do in this case is to measure fixed quadratures on the two modes for a varying quantum state $|\Psi_s^{\phi_i}\rangle$, it is immediate to show that this is equivalent to perform a conventional LO phase scan of the fixed quantum state $|\Psi_s^{\phi_i=const}\rangle$. We shall name this technique as "remote balanced homodyne tomography".

For each value of the interferometer phase φ_{int} and upon detection of an idler photon, stable and fast quadrature measurements have been realized on the corresponding pair of consecutive signal time-bins (plus one containing just the vacuum and used for calibration), while keeping both the local oscillator and the homodyne detection apparatus unchanged. A total of 10^6 quadrature measurements, equally distributed over the range $[0, \pi]$ of φ_{int}, has been performed on each of the three time-bins.

The experimental results are reported in Fig. 2, where we plot the measured values of the quadratures X_1 and X_2 obtained for three different values of the remote relative phase ϕ_i, while leaving $\Delta\theta$ fixed. According to the above reasoning, these results also represent the marginal distributions $p(X_1, X_2, \Delta\theta)$ associated with the ebit of Eq. (2) for $\phi_i = 0$, and obtained for three different values of the relative LO phase $\Delta\theta$.

The results shown in Fig. 2 explicitly show the strong phase-dependence of the joint distribution $p(X_1, X_2, \Delta\theta)$ as opposed to the complete phase-independence of the distributions $p(X_1)$ and $p(X_2)$ associated with each temporal mode, separately. This result is consistent with the fact that each mode, separately, is an incoherent statistical mixture of vacuum and single-photon Fock state; however, the pair of modes 1 and 2, as a whole, is in the coherent superposition described by Eq. (2), with $\phi_i = 0$. Figure 2 also shows that a single-photon Fock state is defined in the phase space $(x_A^{\phi_i=0}, y_A^{\phi_i=0})$, while the vacuum is defined in the phase space $(x_B^{\phi_i=0}, y_B^{\phi_i=0})$, in line with the theoretical prediction of Eq. (6).

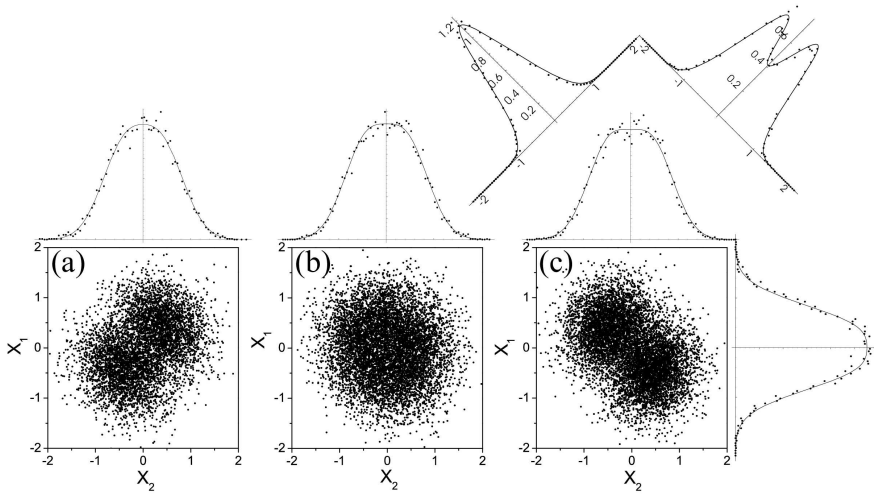

Figure 2. Joint marginal distributions of the measured two-mode field quadratures for: (a) $\phi_i = -\Delta\theta$, (b) $\phi_i = \pi/2 - \Delta\theta$, (c) $\phi_i = \pi - \Delta\theta$, while leaving $\Delta\theta$ fixed. These are also the joint marginal distributions $p(X_1, X_2, \Delta\theta)$ associated with the ebit of Eq. (2) for $\phi_i = 0$, and corresponding, respectively, to $\Delta\theta = 0$, $\pi/2$, π. The histograms are the single-mode marginal distributions $p(X_1)$ and $p(X_2)$ together with the corresponding best fits. The marginals for the $x_{A,B}$ quadratures are plotted on the diagonal axes above (c).

Figure 3 reports the reconstructed density matrix. Due to experimental inefficiencies in both preparation (η_p) and detection (η_d), the measured state is clearly not pure and is rather described by the (incoherent) mixture

$$\hat{\rho} = (1-\eta)|0\rangle_{s\,s}\langle 0| + \eta|\Psi^{\phi_i=0}\rangle_{s\,s}\langle\Psi^{\phi_i=0}|, \tag{7}$$

with the overall efficiency $\eta = \eta_p\eta_d = 60.5\%$ calculated from the $|00\rangle\langle 00|$ element of the experimentally reconstructed density matrix. It is worth mentioning that this efficiency is exactly the same we find when no interferometer is inserted in the idler channel, namely, when a signal single photon is perfectly localized within a given temporal mode. In other words, η represents our inability of producing and detecting a pure single-photon state, but such limited experimental efficiency seems not to affect the coherence of the delocalized single photon (i.e. its degree of entanglement). This is apparent from Fig. 3 where all the density matrix elements associated with the entangled state of Eq. (2) have approximately equal weights: the vacuum contamination, hence the losses, does not degrade the coherence of the remotely delocalized single photon. This may be understood as a consequence of the common losses undergone by the pair of entangled time-bins carrying the single photon.

Figures 4(a) and (b) reproduce, respectively, the $(x_1, y_1; -0.1, -0.1)$ and $(x_1, 0, x_2, 0)$ sections of the two-mode Wigner function $W^{\phi_i=0}(x_1, y_1, x_2, y_2)$ reconstructed from all the density matrix elements appearing in Fig. 3 (i.e., including the vacuum coming from non-unitary experimental efficiency). The cross section in the (x_1, y_1) plane resembles the standard Wigner function of a single-photon Fock state, but is characterized by a well-defined phase; as expected from Eqs. (4) and (5), the specific value of is phase is defined both by the *relative phase* ϕ_i characterizing the single-photon time-encoded ebit and by the point (x_2, y_2) where the cross-section of the 4-D Wigner function is taken. This phase indicates the coherent delocalization of a single photon between two separate temporal modes, which may be interpreted as a sign of single-photon

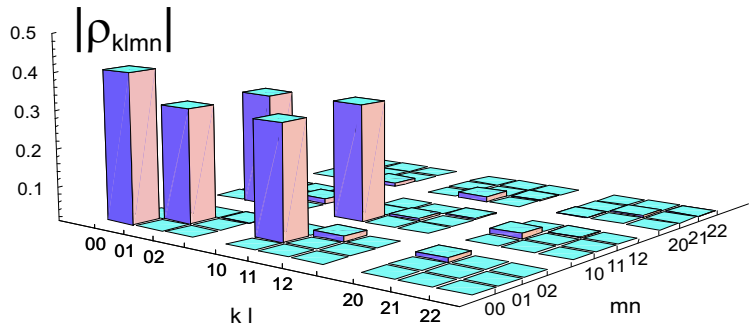

Figure 3. Reconstructed density matrix elements $\rho_{klmn} = \langle k_1 l_2 | \hat{\rho} | m_1 n_2 \rangle$ corresponding to the state of Eq. (2) with $\phi_i = 0$.

two-mode entanglement.The cross section of the two-mode Wigner function $W^{\phi_i=0}(x_1, y_1, x_2, y_2)$ in the (x_1, x_2) plane explicitly shows that correlations exist between the quadratures x_1 and x_2 associated with mode 1 and 2, respectively; again, the non-factorable nature of the remotely prepared delocalized single photon is here apparent.

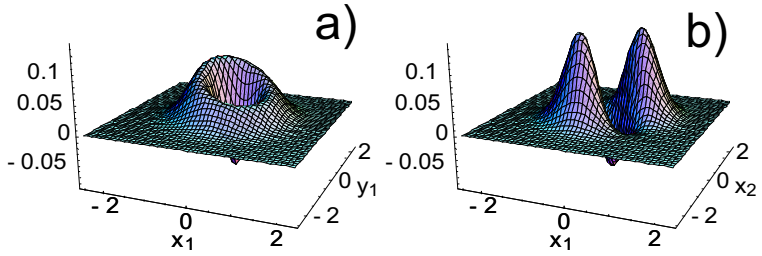

Figure 4. Cross sections of the reconstructed two-mode Wigner function: (a) $W^{\phi_i=0}(x_1, y_1; -0.1, -0.1)$, and (b) $W^{\phi_i=0}(x_1, 0; x_2, 0)$.

Similar to the reconstructed density matrix of Fig. 3, also the reconstructed two-mode Wigner function is affected by the non-unitary experimental efficiency: our overall efficiency $\eta = 60.5\%$ allows observing the negativity of the Wigner function, but this would be much more pronounced for higher values of η.

5 Conclusion

The experimental reconstruction of the density matrix and Wigner function of the conditionally prepared system has enabled us to analyze its purity and coherence. Beside the non-classical behavior typical of single-photon Fock states (negative values around the origin), the reconstructed 4-D Wigner function has been found to be characterized by an intriguing phase information and by correlation between well separated temporal modes, as expected from Eq. (4).

From a corpuscular perspective, it may seem counterintuitive that a single photon simultaneously affects two non-overlapping temporal modes or, equivalently, carries a well defined phase. However, the effect can be understood in terms of the coherent superposition *remotely* induced between otherwise independent *signal* time-bins; in this perspective, the two co-propagating but well-separated signal temporal modes carrying a delocalized single photon can be considered to be entangled.

Following this line of thought, it would be interesting to check whether or not the non-classical correlations we have found between pairs of non-overlapping temporal modes are nonlocal (i.e., violate a Bell-type inequality). The locality criterion recently proposed by Banaszek *et al.* [10] seems to offer this opportunity: the single-photon time-encoded entangled state of Eq. (2 is expected to give rise to a maximal violation of Banaszek-Bell inequality. However, when accounting for the limited experimental efficiencies, we find that a loophole-free test of Banaszek-Bell's inequality would be attainable only for global experimental efficiencies larger than 96%, which is not our case. We are currently investigating how to properly introduce some reasonable auxiliary assumptions in order to overcome this difficulty. Thanks to the high efficiencies

achievable by homodyne detectors and considering that quite high single-photon preparation efficiencies are currently possible, the tomographic approach to Bell's inequality [10] may have the potentials to open the way to a loophole-free test of the nonlocality of a single-photon two-mode entangled state.

From the applicative viewpoint, one of the most interesting aspects of the scheme we have developed is the dependence of the relative phase characterizing the delocalized (signal) single photon on both the relative phase between pump pulses and the phase delay introduced by the remote Michelson interferometer. Based on this effect, for any fixed value of the remotely controlled phase ϕ_i, one may generate, in the signal arm, a specific single-photon ebit. In other words, the proposed scheme can be regarded as a remotely tunable source of arbitrary single-photon ebits; such a source is highly desirable for applications in quantum information technology.

6 Acknowledgments

M.D. thanks A. Garuccio, V.L. Lepore, Y.H. Kim, and Y.H. Shih for stimulating discussions. This work has been performed in the frame of the "Spettroscopia laser e ottica quantistica" project of the Physics Department of the University of Florence and partially supported by Ente Cassa di Risparmio di Firenze, MIUR, under the FIRB contract RBNE01KZ94, and PRIN.

References

[1] A. Einstein, B. Podolsky, and N. Rosen, Phys. Rev. **47**, 777 (1935). J.S. Bell, Physics **1**, 195 (1964).
[2] J.S. Bell, Physics **1**, 195 (1964)
[3] C.H. Bennett, and B.D. DiVincenzo, Nature **404**, 247 (2000)
[4] S.M. Tan, D.F. Walls, and M.J. Collett, Phys. Rev. Lett. **66**, 252 (1991)
[5] S. Giacomini *et al.*, Phys. Rev. A **66**, 030302 (2002); F. Sciarrino *et al.*, Phys. Rev. A **66**, 024309 (2002)
[6] E. Knill, R. Laflamme, and G.J. Milburn, Nature (London) **409**, 46 (2001); N.J. Cerf, C. Adami, P.G. Kwiat, **57**, 1477 (1998); H.-W. Lee, and J. Kim, Phys. Rev. A **63**, 012305 (2001); H.-W. Lee, *ibid.* **64**, 014302 (2001); C.J. Villas-Bôas, N.G. de Almeida, and M.H.Y. Moussa, Phys. Rev. A **60**, 2759 (1999)
[7] T. B. Pittman, B. C. Jacobs, and J. D. Franson, Phys. Rev. A **71**, 032307 (2005)
[8] E. Santos, Phys. Rev. Lett. **68**, 894 (1992); L. Hardy, Phys. Rev. Lett. **73**, 2279 (1994); L. Vaidman, *ibid.* **75**, 2063 (1995); L. Hardy, *ibid.* **75**, 2065 (1995); D.M. Greenberger, M.A. Horne, a. Zeilinger, *ibid.* **75**, 2064 (1995); A. Peres, *ibid.* **74**, 4571 (1995); D. Horne, *et al.*, Phys. Lett. A **209**, 1 (1995); K. Jacobs, *et al.*, Phys. Rev. A **54**, R3738 (1996)
[9] S.A. Babichev, *et al.*, Phys. Rev. Lett. **92**, 193601 (2004)
[10] K. Banaszek, and K. Wodkiewicz, Phys. Rev. A **58**, 4345 (1998); Phys. Rev. Lett. **82**, 2009 (1999)
[11] S. J. Van Enk, Phys. Rev. A **72**, 064306 (2005)
[12] M. Pawlowski and M. Czachor, quant-ph/0507151, and Phys. Rev. A **73**, 042111 (2006)
[13] A. Zavatta, M. D'Angelo, V. Parigi, M. Bellini, Phys. Rev. Lett. **96**, 020502 (2006)
[14] J.D. Franson, Phys. Rev. Lett. **62**, 2205 (1989)
[15] Gisin's group has recently realized (see, e.g., J. Brendel, *et al.*, Phys. Rev. Lett. **82**, 2594 (1999); H. de Riedmatten, *et al.*, Phys. Rev. A **69**, 050304 (2004) and ref. therein) and exploited (W. Tittel, *et al.*, Phys. Rev. Lett. **84**, 4737 (2000), H. de Riedmatten *et al.*, *ibid* **92**, 047904 (2004); I. Marcikic, *et al.*, Nature (London) 421, 509 (2003)) the purely quantum correlations characterizing two-photon systems entangled in $N \geq 2$ ultra-short co-propagating temporal modes (or 'time-bins'). This is an example of two-photon N-mode (or N-time-bin) entanglement: the two photons are in the same spatiotemporal mode and have equal polarization, hence, it is the presence and absence of a photon pair from two or more separate time-bins what generates quantum correlations between the involved time bins. See also C. Simon, and J.-P. Poizat, Phys. Rev. Lett. **94**, 030502 (2005), and references therein.
[16] I.L. Chuang, and Y. Yamamoto, Phys. Rev. Lett. **76**, 4281 (1996)
[17] D.N. Klyshko, *Photon and Nonlinear Optics*, Gordon and Breach Science, New York, 1988
[18] T.E. Keller, and M.H. Rubin, Phys. Rev. A **56**, 1534 (1997); Y.-H. Kim *et al.*, Phys. Rev. A **62**, 043820 (2000); A.V. Burlakov, M.V. Chekhova, O.A. Karabutova, S.P. Kulik, Phys. Rev. A **63**, 053801 (2001) Y.-H. Kim, M.V. Chekhova, S.P. Kulik, and Y.H. Shih, Phys. Rev. A **60**, 37 (1999);
[19] D.N. Klyshko, Phys. Lett. A 128, 133 (1988), *ibid* 132, 299 (1988)
[20] A. Zavatta, M. Bellini, P. L. Ramazza, F. Marin and F. T. Arecchi, J. Opt. Soc. Am. B 19, 1189 (2002)
[21] A. Zavatta, S. Viciani, and M. Bellini, Phys. Rev. A **70**, 053821 (2004)
[22] T. Aichele, A.I. Lvovsky, and S. Schiller, Eur. Phys. J. D **18**, 237 (2002)
[23] M. Bellini, F. Marin, S. Viciani, A. Zavatta, F.T. Arecchi, Phys. Rev. Lett. **90**, 043602 (2003)
[24] S. Viciani, A. Zavatta, and M. Bellini, Phys. Rev. A **69**, 053801 (2004)
[25] A. Zavatta, S. Viciani, and M. Bellini, Science **306**, 660 (2004); and Phys. Rev. A **72**, 023820 (2005)
[26] U. Leonhardt, *Measuring the Quantum State of Light*, Cambridge University Press, Cambridge, 1997
[27] G.M. D'Ariano, C. Macchiavello, and M.G.A. Paris, Phys. Rev. A **50**, 4298 (1994); G.M. D'Ariano in *Quantum optics and Spectroscopy of Solids*, edited by T. Hakioglu and A. Shumovsky (Kluwer Academic, Dordrecht, 1997), pp. 175-202